Soils and Foundations 2014;54(4):560–572

HOSTED BY
ELSEVIER

CrossMark

The Japanese Geotechnical Society

Soils and Foundations

www.sciencedirect.com
journal homepage: www.elsevier.com/locate/sandf

The impact of the 2011 Tohoku earthquake tsunami disaster and implications to the reconstruction

Shunichi Koshimura[a,*], Satomi Hayashi[b], Hideomi Gokon[b]

[a]International Research Institute of Disaster Science, Tohoku University, Aoba 6-6-03, Aramaki, Aoba-ku, Sendai 980-8579, Japan
[b]Graduate School of Engineering, Tohoku University, Aoba 6-6-03, Aramaki, Aoba-ku, Sendai 980-8579, Japan

Received 24 July 2012; received in revised form 17 January 2014; accepted 3 February 2014
Available online 22 July 2014

Abstract

The authors conducted a comprehensive study to identify the impact of the 2011 Tohoku tsunami disaster and to understand the lessons towards the reconstruction of Tohoku to build tsunami-resilient community. First, the authors identified the extent of tsunami inundation zone by field measurement and satellite remote sensing. A specific index for optical satellite images was applied for the extraction of tsunami inland penetration calibrated with the ground truth data (field survey data). Second, an integrated investigation of field measurement and aerial photo and video inspections with spatial information sciences was performed to understand the hydrodynamic aspect of tsunami inland penetration with a form of tsunami flow velocity and hydrodynamic force, and the preliminary results lead to new understandings of structural vulnerability against the 2011 tsunami with a form of tsunami fragility curve and an implication for land use management and relocation planning to reconstruct resilient coastal communities.

Keywords: The 2011 Tohoku earthquake and tsunami; Remote sensing; GIS; Structural vulnerability; Fragility curve; Numerical modeling

1. Introduction

On 11 March, 2011, a devastating tsunami accompanied with M9.0 earthquake attacked the northern Pacific coast of Japan, and the coastal communities especially in Iwate, Miyagi, and Fukushima Prefectures were totally devastated. The total affected area by the tsunami was reported as 561 km^2 along the Pacific coast of Japan (Geospatial Information Authority of Japan (GSI), 2011a), and the maximum tsunami run-up height reached up to 40 m in Iwate Prefecture (Mori et al., 2011). As of 27 June 2012, National Police Agency reported 15,866 dead (4671 in Iwate, 9523 in Miyagi, and 1606 in Fukushima) and 2946 missing, 130,441 buildings/houses were collapsed or washed-away (National Police Agency, 2011). The economic impacts were estimated as 16–25 trillion yen (Cabinet Office, http://www.bousai.go.jp/oshirase/h23/110624-1kisya.pdf), while FY2011 national budget of Japan was 92 trillion yen (Ministry of Finance Japan, 2011).

Having passed more than two years since the event occurred, the devastated areas started moving forward to reconstruct their communities. Approximately 82,000 residents who lost houses moved from shelters to temporary houses (supplied 53,000 units) and rental housing (Ministry of Land, Infrastructure, Transport and Tourism, 2011). Though the recovery process is still underway, local governments

*Corresponding author.
E-mail address: koshimura@irides.tohoku.ac.jp (S. Koshimura).
Peer review under responsibility of The Japanese Geotechnical Society.

http://dx.doi.org/10.1016/j.sandf.2014.06.002
0038-0806/

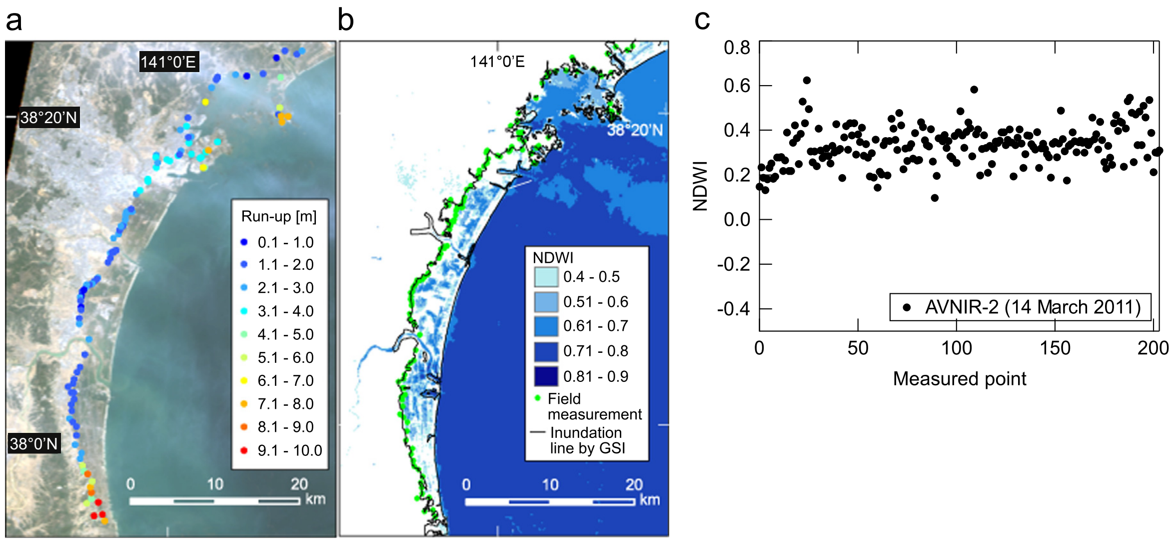

Fig. 1. (a) ALOS AVNIR-2 image of Sendai plain, acquired on 14 March 2011 with the measurement of the run-up heights at tsunami inundation limit (Abe and Abe, 2011). The datum line is Tokyo Peil (T.P.). (b) Spatial distribution of NDWI for mapping tsunami inundation extent. Green dots are the survey points of tsunami inundation extent used for thresholding of NDWI-0.4. Black solid line indicates the inundation limit surveyed by Geospatial Information Authority of Japan (GSI) (2011a). (c) Distribution of NDWI from ALOS/AVNIR-2 image sampled along the tsunami inundation limit. (For interpretation of the references to color in this figure caption, the reader is referred to the web version of this paper.)

completed the draft of reconstruction plan including infrastructure design, transportation, land use management, urban design, relocation, and economic and industrial outlooks.

This paper aims to summarize the impact of the 2011 Tohoku tsunami disaster with particular regard to structural damage, to understand the lessons towards reconstruction of Tohoku region. To identify the tsunami impact, we conducted an integrated studies of field measurement, satellite image analysis, aerial photo inspection with the approach of spatial information sciences. The findings lead to understanding structural vulnerability against the 2011 tsunami and provide an implication for land use management and relocation planning to reconstruct resilient coastal communities.

2. Extracting tsunami inundation zone by optical satellite images

2.1. Field survey

The significant feature of the 2011 tsunami was the wide extent of inundation zone. In fact, on the Sendai plain, the tsunami inundated more than 5 km inland to have caused total devastation and the tsunami inundation on the Sendai plain remained for several days because of the wide-area subsidence (Imakiire and Koarai, 2012). Since the event occurred, many Japanese groups have conducted emergency field surveys to measure the tsunami inundation and run-up heights, flow depths. Our group focused on mapping the inundation limit of the coast of Tohoku region to understand how the tsunami left the wide extent of the impacted areas. We conducted high-resolution surveys of the inundation limits and heights in the few-centimeter accuracy by using RTK-GPS measurement system (Promark 3) in Miyagi, Iwate, and Aomori Prefectures (Abe and Abe, 2011). The horizontal measurement interval is ranging from approximately 500 m to several kilometers and we measured nearly 300 sites until the end of April 2012 (Fig. 1(a)).

2.2. Tsunami inundation zone estimated from ALOS/AVNIR-2 image

In 2006, the Japan Aerospace Exploration Agency (JAXA) launched the satellite, Advanced Land Observing Satellite (ALOS), which has been developed to contribute to the fields of mapping, precise regional land coverage observation, disaster monitoring, and resource surveying. ALOS was loading three types of sensors: the Panchromatic Remote-sensing Instrument for Stereo Mapping (PRISM); the Advanced Visible and Near Infrared Radiometer type 2 (AVNIR-2), which observes land covers; and the Phased Array type L-band Synthetic Aperture Radar (PALSAR), which enables day-and-night and all-weather land observation. Unfortunately, on 12 May 2012, ALOS completed its operation after 6.5 million scenes of image acquisition for five years (Japan Aerospace Exploration Agency (JAXA), 2011). After the 2011 Tohoku earthquake, ALOS captured whole part of Sendai plain, approximately 500 km^2 from Sendai city to the south of Yamamoto town, Miyagi Prefecture. We used the post-event image of AVNIR-2 data which was released immediately after the acquisition, 14 March 2011. This image was significantly contributed to quick understanding of the tsunami inundation extent (Rao and Lin, 2011).

Here, mapping tsunami inundation extent was conducted through the analysis of AVNIR-2 image with the ground truth calibration from the field survey. A unique feature of tsunami inundation zone is the sea water penetration on land. Thus, the optical satellite remote sensing for mapping tsunami affected area focuses on extracting water body from the post-event image. Here, we introduced the Normalized Difference Water

Index (NDWI) to extract the inundated area. In general, NDWI uses two bands of green, blue, NIR and SWIR according to the purpose of extraction (Gao, 1996; McFeeters, 1996; Xu, 2006; Lei et al., 2009). Here, we particularly used blue and NIR bands to calculate NDWI, as shown in Eq. (1), for the purpose of mapping the tsunami inundation zone with the threshold values obtained from the ground observation:

$$\mathrm{NDWI} = \frac{B - NIR}{B + NIR} \quad (-1 \leq \mathrm{NDWI} \leq 1) \tag{1}$$

where B and NIR are the radiance values of visible blue and near infrared bands, respectively.

Fig. 1 shows the true color composite of the 14 March 2012 ALOS AVNIR-2 image with field measurement of the tsunami inundation extent and the result of the extraction of the tsunami inundation zone. Through trial and error, we found that NDWI ≥ 0.4 was most consistent with the measured inundation limit (black dots of our measurement), for mapping the tsunami inundation zone. Theoretically, NDWI varies from -1 to 1 according to the spectral features of ground surface objects. Especially, water, which strongly reflects blue wavelength and absorbs NIR light/radiation, shows higher value of NDWI. In this study, the analysis is performed on the assumption that the NDWI values in the inundated areas are higher because of the existence of water and they suddenly decrease on the dry land through the boundary of the inundation limit. This is the basic idea we determine for the threshold value in NDWI to extract the inundated areas.

To determine the NDWI threshold, we used the result of the field survey measuring the position of the inundation limit (Abe and Abe, 2011). Fig. 1(c) shows the variation of NDWI from ALOS/AVNIR-2 image sampled along the inundation limit. The average value of NDWI at all the points of measurement was 0.34. Note that we started the field survey on the next day of the tsunami attack until the end of April 2011 and the tsunami inundation limit would be found through inspecting the existing water edge, littered debris, deposited sediments and interviewing with eyewitnesses. Through trial and error of mapping NDWI from ALOS/AVNIR-2 image, we determined the threshold value as NDWI = 0.4 to be most consistent with the measured inundation limit. Then, the results of the extraction of the tsunami inundation zone were verified through the comparison with the visually inspected inundation line by Geospatial Information Authority of Japan (GSI) (2011a).

3. Mapping structural damage and vulnerability

3.1. Visual inspection of aerial photos

After extracting the tsunami inundation zone, mapping structural damage was conducted through visual interpretation of aerial photos to identify the structural vulnerability against the 2011 tsunami. For visual inspection, we used the aerial photo archives of Geospatial Information Authority of Japan (GSI) (2011b) acquired in the devastated area. The ortho photos of 80 cm/pixel resolution were composited with mosaic image processing. Combined with the ZENRIN building data (building shape files), the inspection was conducted for each building by comparing pre- and post-tsunami aerial photos

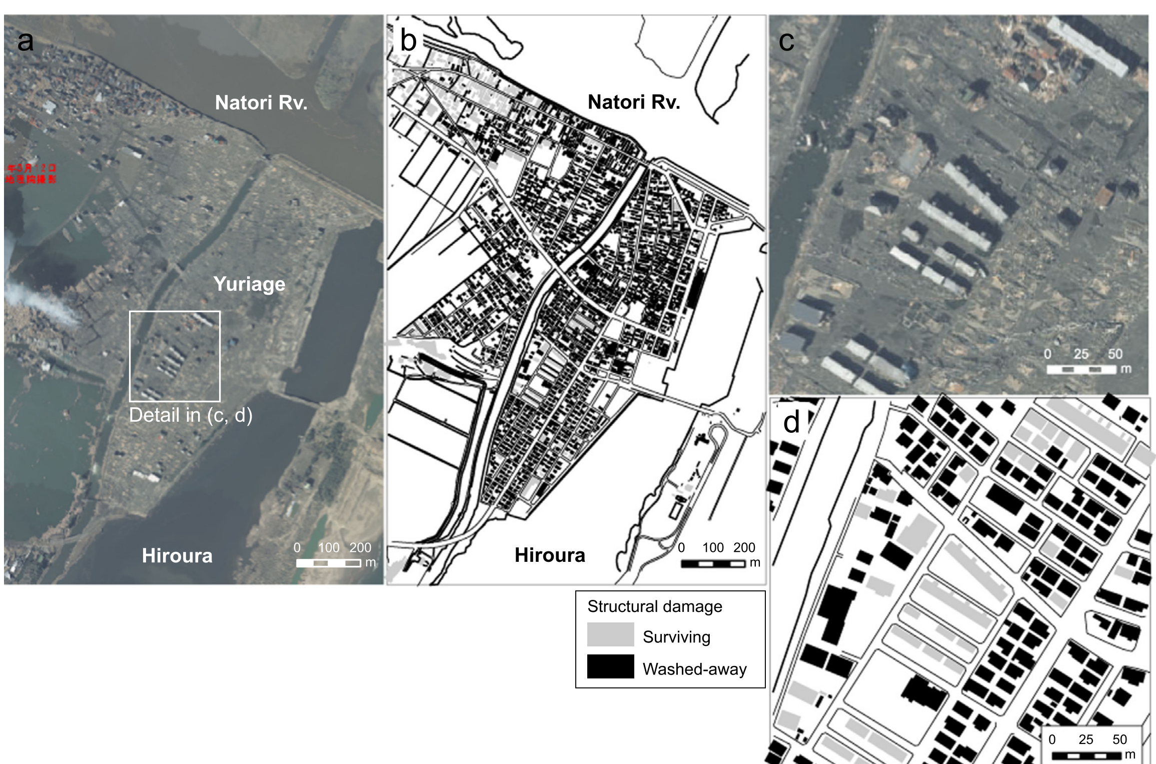

Fig. 2. Example of mapping structural damage in Yuriage, Natori city, by inspection of post-event aerial photos.

focusing on the existence of houses' roofs to add an attribution of classification “washed-away” or “surviving” as the damage status. Note that there is no account of building construction type in the dataset we prepared. Further analysis is now underway to determine the structural vulnerability for each structural type.

Fig. 2 shows an example of the classification in Yuriage, Natori city. The result of mapping of structural damage in Miyagi Prefecture is summarized in Table 1 and the mapping results are in our web site[1] to be used for field survey, land use management to understand vulnerable areas and reconstruction planning.

Combined with the results of mapping inundation zone, structural damage classification results enable to determine the number of exposed structures, then calculate P_D, the proportion of the number of structure classified as “washed-away” and the number of exposed structure. Table 1 implies that almost 30 % of the structures in the tsunami inundation zone in Miyagi Prefecture were devastated and a high proportion of devastated buildings is concentrated in the northern part of Miyagi Prefecture (Sanriku region). Sanriku coastline is particularly vulnerable to tsunamis, because it has many V-shaped bays that cause tsunami energy to converge and amplify. In addition, the death ratio, which was obtained as a proportion of the number of death and exposed population, shows somehow correlation with P_D. Surprisingly, 12.2% of the population in Onagawa town were killed by the tsunami. This implies that Onagawa town was difficult to survive under the attack of the tsunami of approximately 20 m.

Table 1
Proportion of devastated buildings in the tsunami inundation zone and fatalities in coastal municipalities in Miyagi Prefecture. The number of fatality is based on the report of the Statistics Bureau (as of 24 October, 2010). The table is modified from the original one (Gokon and Koshimura, 2012) to add the fatality ratio.

Municipality	Exposed structure	Washed-away	P_D (%)	Fatality	Fatality ratio (%)
Kesennuma city	13,951	8047	57.7	1404	3.5
Minamisanriku town	6665	5418	81.3	902	6.3
Onagawa town	4607	3459	75.1	980	12.2
Ishinomaki city	62,440	12,521	20.1	3892	3.5
Higashimatsushima city	16,860	3171	18.8	1138	3.3
Shiogama city	8995	373	4.1	21	0.11
Matsushima town	695	14	2.0	2	0.05
Rifu town	187	8	4.3	46	8.5
Shichigahama town	3253	1120	34.4	75	0.82
Tagajo city	6310	226	3.6	189	1.1
Sendai city	13,721	4329	31.6	730	2.4
Natori city	5530	2810	50.8	981	8.1
Iwanuma city	5285	1298	24.6	183	2.3
Watari town	8143	2059	25.0	270	1.9
Yamamoto town	5373	2802	52.0	690	7.7
Total	162,015	47,655	29.4	9439	2.8

3.2. Structural vulnerability and tsunami fragility curves

Integrating structural damage mapping with field survey data, such as flow depths, leads to a new measure of identifying structural vulnerability against tsunami, as a form of tsunami fragility curve or tsunami fragility function. Tsunami fragility curve is defined as the structural damage probability or fatality ratio with particular regard to the hydrodynamic features of tsunami inundation flow, such as flow depth, current velocity and hydrodynamic force (Koshimura et al., 2009a, 2009b).

In the hydrodynamic parameters of developing tsunami fragility curves, only the maximum flow depth can be obtained in the field measurement. Fig. 3 shows the spatial distribution of flow depths measured in tsunami inundation zone (Koshimura and Gokon, 2012). Spatial interpolation of measurement data (point data) to obtain raster data is combined with the structural damage mapping (e.g. Fig. 2). The procedure of developing tsunami fragility curves is as follows:

1. *Damage data acquisition*: Obtaining damage data from aerial photo interpretation.
2. *Tsunami hazard estimation*: Estimating the hydrodynamic features of tsunami by field measurement.
3. *Data integration between the damage data and tsunami hazard information*: Correlating the damage data and the hydrodynamic features of tsunami through the GIS analysis.
4. *Calculating damage probability*: Determining the damage probabilities by counting the number of damaged or survived structures, for each range of flow depths.
5. *Regression analysis*: Developing the fragility curves by regression analysis of discrete sets of damage probability and hydrodynamic features of tsunami.

Taking the above procedure, the tsunami fragility curve is preliminary obtained as shown in Fig. 4. The fragility curve shown in the figure indicates the damage probabilities of structural destruction equivalent to the flow depth. Structures in Miyagi Prefecture were especially vulnerable when the local flow depth exceeded 2 m, and 6 m flow depth would totally cause total devastation. The plot of Fig. 4 also includes the tsunami fragility curve in Banda Aceh, Indonesia for a comparison (Koshimura et al., 2009a). The fragility curve from Banda Aceh was obtained by integration of satellite image interpretation and the numerical analysis of tsunami inundation. Interestingly, these two curves show a similar characteristic when the flow depth is less than 2 m, and structures in Banda Aceh are more vulnerable when the maxim flow depth is higher than 3 m. However, we have not yet identified how this difference has occurred. The major structure types in Banda Aceh were low-rise wooden house, timber construction, and non-engineered RC construction which is lightly reinforced (Koshimura et al., 2009a), and all of the structural types in the tsunami affected area ware included in Banda Aceh tsunami fragility curve. Further analysis is required to characterize the fragility curves by considering structural type, structural age and urban configurations. In both cases, we can

[1] http://www.tsunami.civil.tohoku.ac.jp

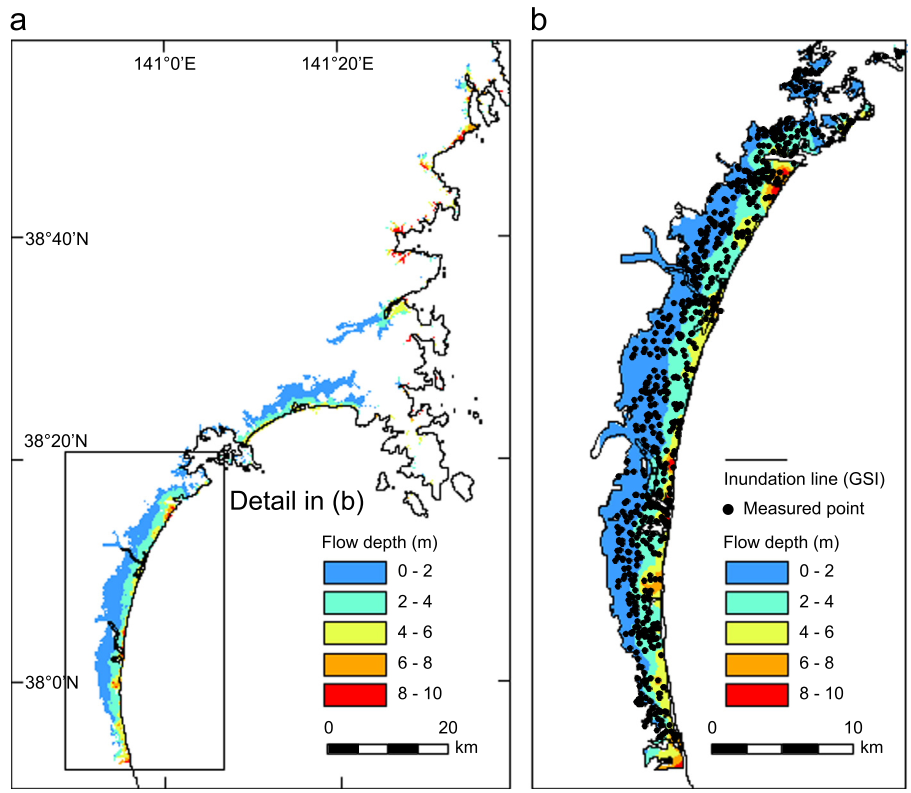

Fig. 3. Mapping the tsunami flow depth measured by Miyagi Prefectural government and our survey team (Abe and Abe, 2011). Black dots indicate the measured points.

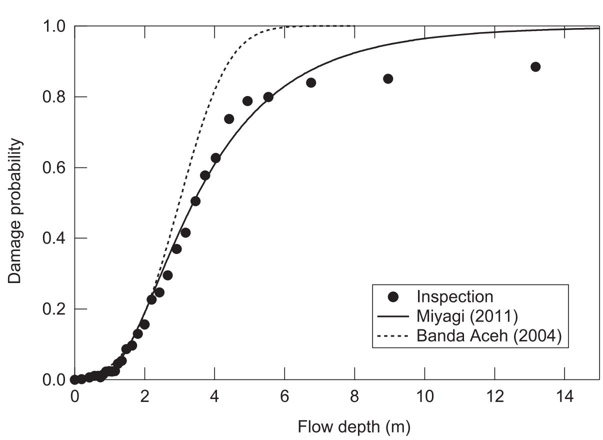

Fig. 4. Tsunami fragility curves for structural destruction (washed-away). The solid line is obtained from Miyagi Prefecture (2011 event) and the dashed one is from Banda Aceh, Indonesia (2004 Indian Ocean tsunami) (Koshimura et al., 2009a).

preliminarily conclude that over 2 m tsunami flow depth may devastate the houses and buildings and this fact leads to a lesson to determine the land use plan (zoning) which considers the effect of coastal protection.

4. Tsunami flow measurement using the video records

4.1. Measuring the tsunami flow velocity

When a tsunami reaches the coast, its characteristics change significantly from water wave to strong water flow. And this strong inundation flow causes damage on infrastructures, buildings and humans. Measuring flow velocities of tsunami inundation on land was quite rare and it was difficult to understand what really happened in the devastated area and to identify the cause and mechanisms of structural destruction by tsunami inundation flow. But in recent years, owing to the handy video cameras and mobile phones, many of tsunami survivors attempted to capture the moment of tsunami attack to their communities and uploaded to the Internet. Applying a video analysis technique, the tsunami flow velocity can be determined.

Here, we acquired two kinds of video data recorded in Miyagi Prefecture (Fig. 5). One is the aerial video taken from NHK's (Japan Broadcasting Corporation) helicopter which has been flying over Natori city, Miyagi Prefecture at the time of tsunami attack. This video has been broadcasted many times in the world and a part of it is on NHK's video archive.[2] The other is a survivor's video that was taken from the roof of the building in Onagawa town, Miyagi Prefecture. A part of this video was uploaded to the web site of Japanese newspaper company, Yomiuri Shinbun.[3] Both captured the moment of tsunami attack and contained important information of how the tsunami penetrated inland and local tsunami inundation flow characteristics.

[2]http://www9.nhk.or.jp/311shogen/map/#/evidence/detail/D0007030024_00000

[3]http://www.yomiuri.co.jp/stream/sp/earthquake/earthquake_088.htm

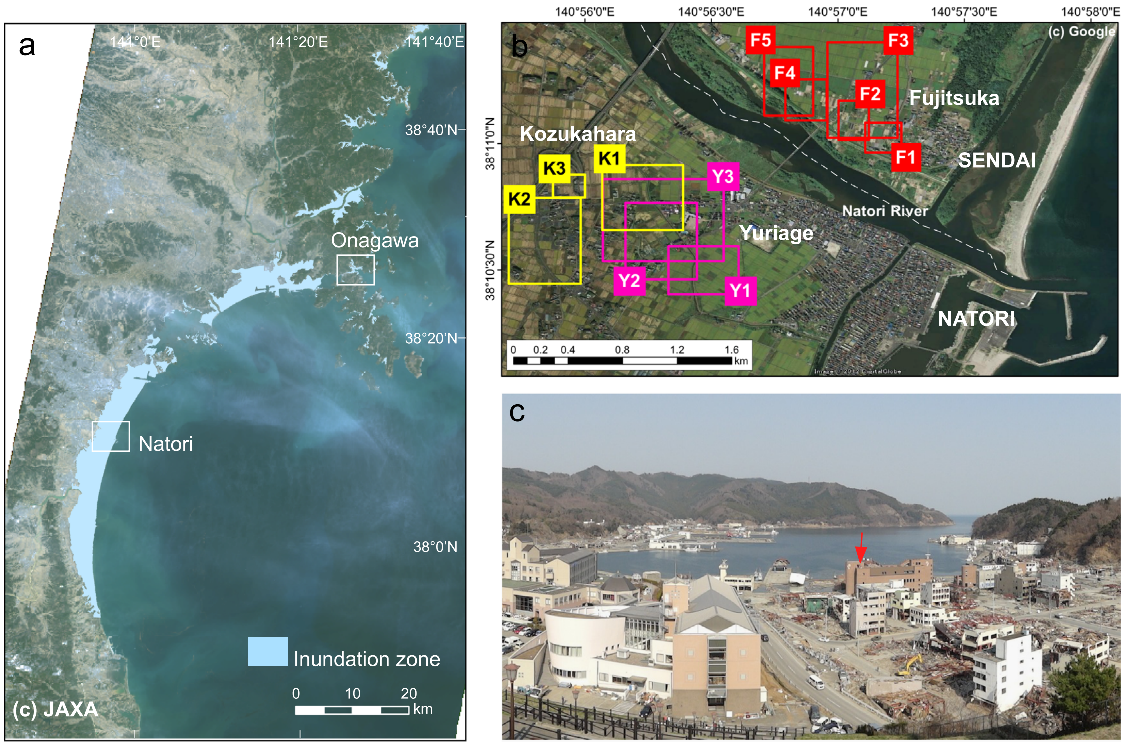

Fig. 5. (a) Map of the study area for tsunami flow velocity measurement. One is from Natori city where NHK's helicopter video was taken and the other is from Onagawa town (survivor's video). (b) Approximate area where the NHK's helicopter video was taken. (c) Overview of Onagawa town. The red arrow indicates the location where the video was recorded. (For interpretation of the references to color in this figure caption, the reader is referred to the web version of this paper.)

4.2. Mapping tsunami penetration using the aerial video

Immediately after the earthquake occurred, NHK (Japan Broadcasting Corporation) sent a crew to Sendai coast on a helicopter to broadcast the tsunami attack. The tsunami arrived at Sendai coast approximately 1 h after the earthquake and NHK crew succeeded to shoot the moment of tsunami attack at the Sendai coast. As shown in Fig. 5(b), they have been flying along Natori river and witnessed the tsunami penetration and run-up along the river.

Fig. 6 shows the procedure for mapping tsunami front (Hayashi and Koshimura, 2013). First, we divide the continuously recorded video into an individual frame. Then the video frames are calibrated and rectified by 2-D projective transformation as defined by Eqs. (2) and (3), with ground control points which could be identified in pre-event Google map and image:

$$i = \frac{a_1 x + a_2 y + a_3}{a_7 x + a_8 y + 1} \quad (2)$$

$$j = \frac{a_4 x + a_5 y + a_6}{a_7 x + a_8 y + 1} \quad (3)$$

where (i, j) is the co-ordinate in the original image, e.g. pixel number, (x, y) is the transformed co-ordinate (in meters), and a_x is the unknown parameter. Finally, each projected frame with the time stamp is stored as one of GIS layers. On each projected frame, the tsunami front was mapped by connecting the points which could be visually identified as tsunami front.

As shown in Fig. 6(c), the time series of tsunami wave front on land was obtained. When the distance between two tsunami front lines is divided by the time, the "tsunami front velocity" can be estimated. In addition, when we focus on the movement of floating objects in the video, the "tsunami flow velocity" can be identified.

Fig. 7 is the mapping result regarding the sequence of the 2011 tsunami front on Sendai plain and the result of measuring the tsunami front velocity. The result of measurement is summarized in Table 2 and Fig. 8. Table 2 indicates the comparison of the present result with that of EERI reconnaissance team (Chock et al., 2012), and both are very consistent. From Fig. 8, the tsunami front and flow velocities reached approximately 8 m/s within 1 km inland from the shoreline, and they decreased as penetrating more into inland. And we also found that the tsunami front velocities were affected by the existence of the structures which reduce the speed of inland tsunami penetration.

4.3. Tsunami flow velocity and hydrodynamic force on buildings interpreted from the survivor video

Here, the authors represent one more example from Onagawa town, Miyagi Prefecture (10,014 population before the earthquake), which is one of the devastated towns by the 2011 Tohoku earthquake tsunami (Fig. 9). The tsunami attacked the town of Onagawa at 15:20 (35 min after the earthquake occurred) and caused 816 fatalities and 125 still missing. As the authors investigated, at least 6 reinforced concrete or steel

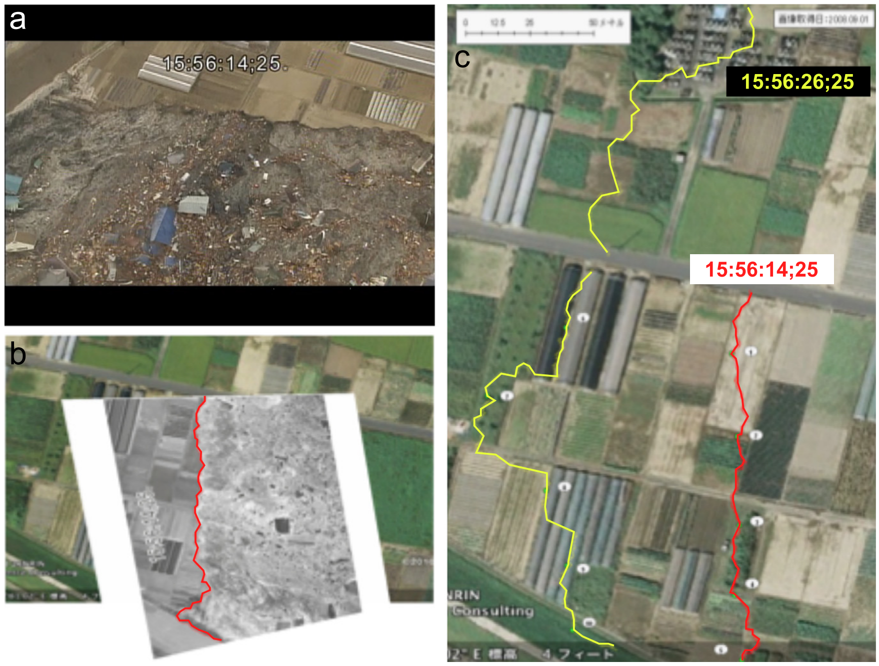

Fig. 6. Procedure of capturing tsunami front from the video. (a) A frame divided from the original video at 15:56:14 (Hours:Minutes:Seconds, 11 March 2011, JST). (b) Result of projective transformation of the captured image. (c) Result of mapping tsunami front captured from the video.

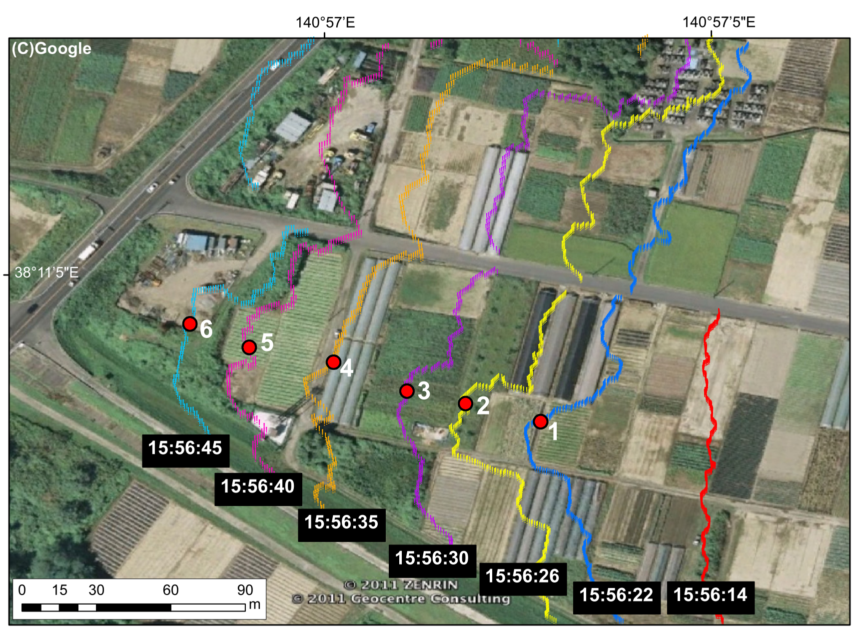

Fig. 7. The sequence of the 2011 tsunami front on Sendai plain and the result of measuring the tsunami front velocity. The red dots are the point of measurements (see Table 2).The captured area is Fujitsuka (F3 in Fig. 5(b)). (For interpretation of the references to color in this figure caption, the reader is referred to the web version of this paper.)

construction buildings were found overturned or washed away. The video was taken by a resident from the top of the reinforced concrete building in Onagawa harbor (Fig. 5(a)). Fig. 10(a) indicates a snapshot from the video capturing the moment of the houses being washed away. Using this video, the author analyzed the time series of flow depth by measuring the height of the water level on withstanding buildings in the video (Fig. 10(b)). Also focusing on the movement of drifting objects, the flow velocity was estimated at the moment when the houses were washed away. As a result, the flow velocity of the tsunami inundation was estimated as 6.3 m/s at the flow depth of approximately 5 m. Using this hydrodynamic

Table 2
The tsunami front velocities estimated from the aerial video analysis and the comparison with the measurements by EERI reconnaissance team (Chock et al., 2012). See Fig. 7 for the location of the measurement. The unit is m/s.

Point (see Fig. 7)	Tsunami front vel. (this study)	Tsunami front vel. (EERI, Chock et al., 2012)
1–2	6.37	6.53
2–3	5.07	5.35
3–4	5.27	4.81
4–5	6.12	5.64
5–6	4.02	4.30

features, the tsunami force was roughly estimated as 100 kN/m, the drag force acting on a wall per unit width.

5. Evaluation of reconstruction plan

In April 2011, one month after the event occurred, the central government established the reconstruction policy council to develop a national recovery and a reconstruction outlook for tsunami-resilient community. Besides, the central government decided the policy of coastal protection, such as seawalls and break waters, which would be designed to ensure their performance to potential tsunami level of approximately 150-year recurrence interval. In this sense, the government policy of designing coastal protection is for 150-year tsunami level (this is called "Prevention Level") which ensures to protect lives and properties. And for the tsunami level more than 150-year recurrence interval, the so-called extreme event, the government calls "Preparedness/Mitigation Level" to reduce the losses and damage by all of the efforts of coastal protection, urban planning, evacuation, and public education.

When the proposed reconstruction plan should be verified, numerical model becomes a powerful tool. We perform the numerical modeling of tsunami inundation in Sendai city by assuming the source model proposed by the authors (Koshimura et al., 2013). A set of non-linear shallow water equations are discretized by the Staggered Leap–frog finite difference scheme with bottom friction in the form of Manning's formula according to the land use condition (Koshimura et al., 2009a). The inundation model results are validated through the comparison with field data in terms of the local inundation depths and inundation heights (Mori et al., 2011).

Fig. 11 shows the result of numerical modeling of the 2011 tsunami inundation in Sendai city (maximum flow depth). After the event occurred, the authors attempted to understand how the tsunami inundated to the Sendai coast by the tsunami inundation modeling using a 10 m topography grid. As shown in the figure, the tsunami penetrated more than 5 km inland to have caused devastation on the coast and to be consistent with the observed tsunami inundation extent. After several aspects of validations (Koshimura et al., 2009a) the tsunami numerical

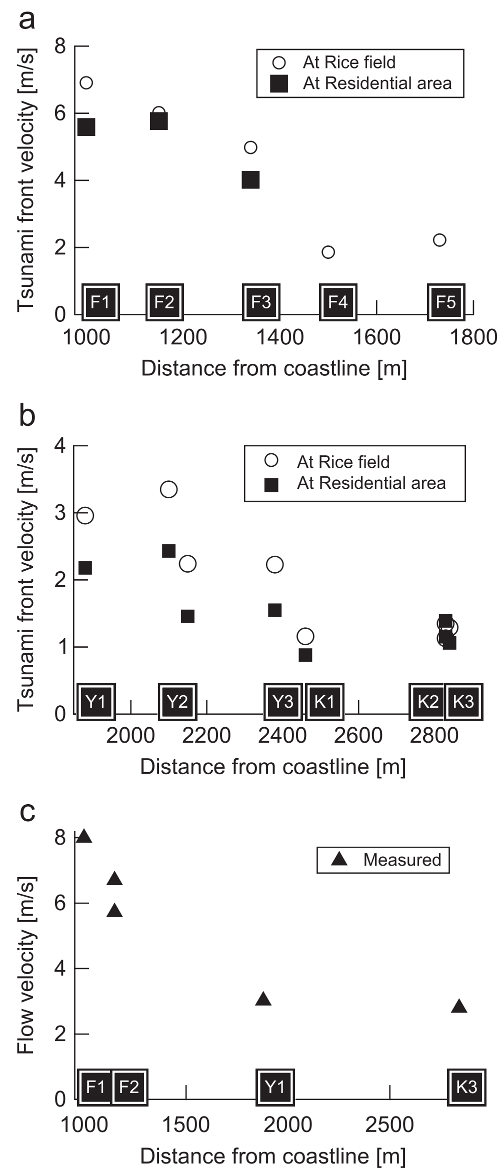

Fig. 8. The result by the tsunami front and flow velocity measurements. (a) Tsunami front velocities in Fujitsuka (the north of Natori river). The tsunami front and the flow velocities were measured in the rice field and residential areas, and the results are plotted with regard to the distances from the coastline. (b) Tsunami front velocities in Yuriage and Kozukahara. (c) The tsunami flow velocities. The annotations F1–F5 (Fujitsuka), Y1–Y3 (Yuriage), and K1–K3 (Kozuhara) indicate the areas where the video images were taken (see Fig. 5(b)).

models can be used for evaluation of reconstruction plans from the view point of tsunami disaster mitigation.

Under the limitations and uncertain conditions of funding, prefectural and local governments have developed their own recovery and reconstruction plans, which assume 10 years to be completed. These plans consist of the combination of structural prevention/mitigation, urban planning, preparedness, and suggest their land use management, relocation, housing reconstruction and tsunami disaster mitigation plans. The key role of academia, in engineering point of view, is to verify and

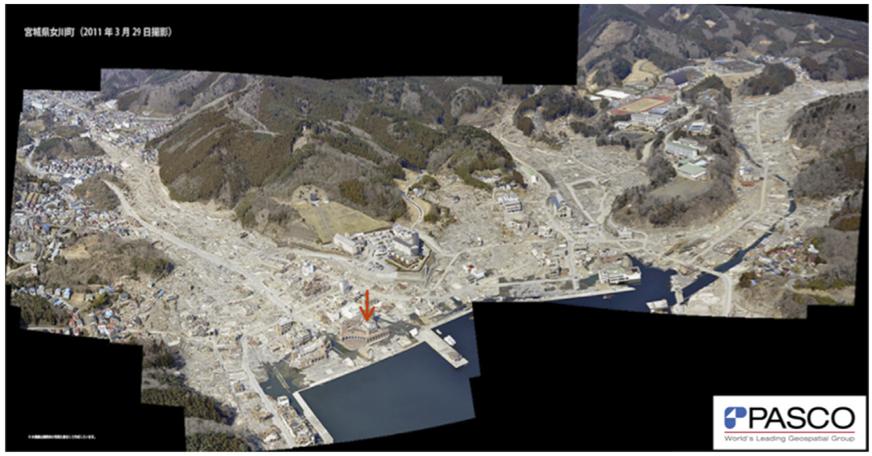

Fig. 9. An overview of Onagawa town, Miyagi Prefecture. Photo taken by PASCO Corporation. The red arrow indicates the point where the survivor video was taken.

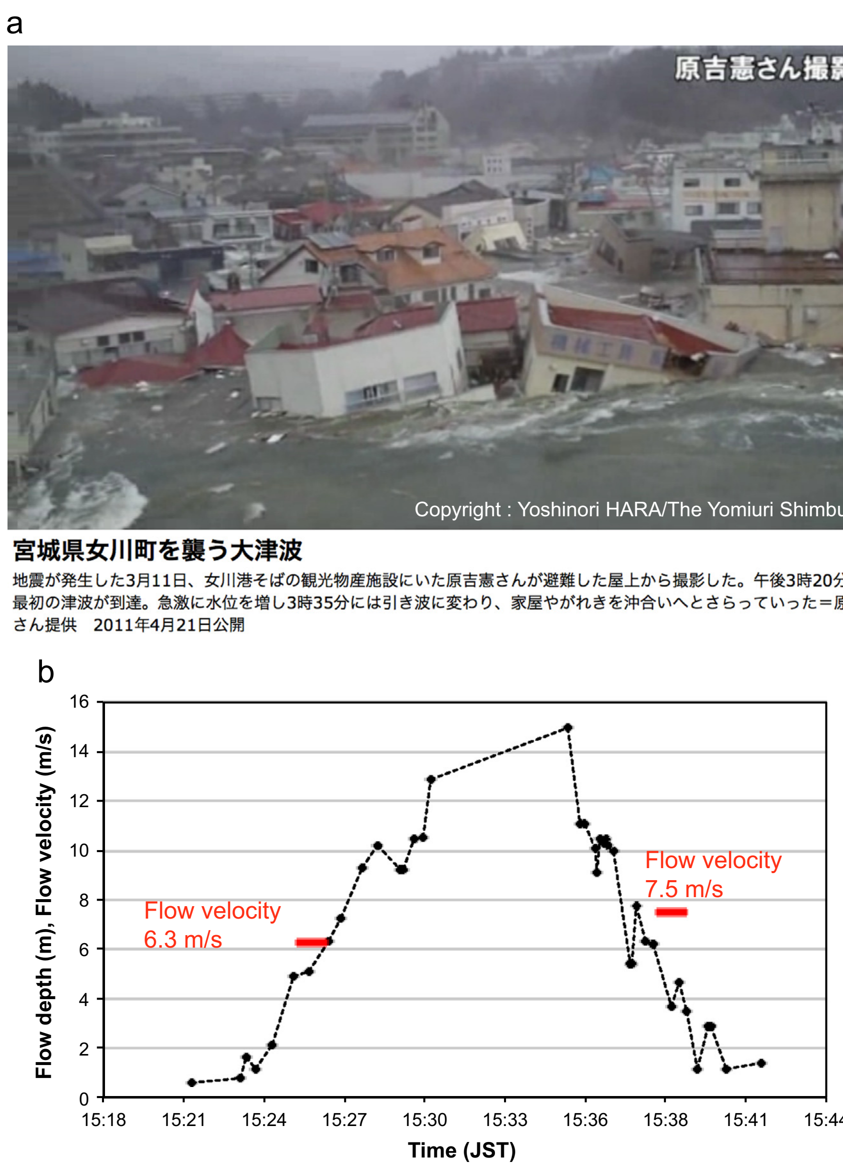

Fig. 10. (a) A snapshot from the survivor video (Yomiuri Shinbun, 2011) capturing the moment that the houses were washed away (approximately at 15:25 JST) (Yomiuri Shinbun, 2011). (b) Time series of tsunami flow depth and flow velocities interpreted by the video.

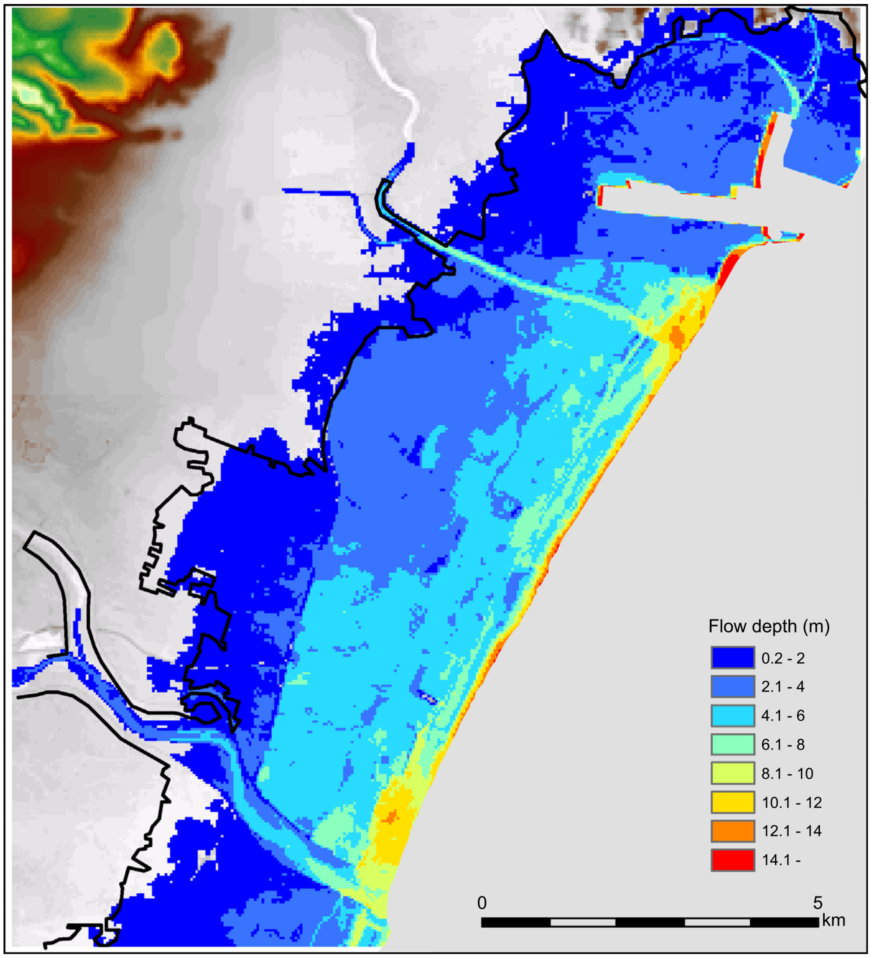

Fig. 11. The result of numerical modeling of the 2011 tsunami inundation in Sendai city (maximum flow depth). Black solid line is the tsunami inundation extent obtained by GSI (2011a).

evaluate if these plans really work for future disaster reduction. For instance, based on the findings regarding the structural vulnerability (see Fig. 4), Sendai city determined a reconstruction plan (Sendai city, 2011) to reduce the tsunami flow depth less than 2 m in the populated area with a conceptual image of multiple coastal protection (Fig. 12(a)). A significant feature of the Sendai city's reconstruction plan is integrating several coastal protection facilities such as seawalls, coastal forests, park (artificial hill) and elevated roads to minimize the potential losses. Fig. 12(b) indicates the plan view of the multiple protection of Sendai city with a 7.2 m seawall and river dike and 6 m elevated prefectural road.

The authors conducted a tsunami numerical modeling under the 2001 tsunami source scenario, by incorporating the reconstruction plan, to evaluate how these protection will work in terms of tsunami reduction. Fig. 13 shows one example from preliminary results. As indicated in the figure, we found that the multiple protection will contribute on substantial reduction of the tsunami inundation zone, and flow depth on Sendai plain especially at the western side of 6 m elevated prefectural road. Using this result, Sendai city determined the land used plan and the area of housing reconstruction and relocation. However, note that the tsunami (the 2011 scenario) will overtop even 7.2 m seawall and the 6 m elevated road. Here, the model assumes no destruction of structures. In this sense, the model cannot reproduce all the aspects of tsunami inland penetration. Coastal infrastructure such as breakwaters and seawalls cannot always protect life and property. Seawalls or coastal structures should be designed with the assumption of overtopping and resiliency, and communities should not rely on coastal infrastructures alone for protection.

6. Summary, towards tsunami-resilient coastal communities

Throughout the comprehensive studies based on the remote sensing, numerical models and spatial information sciences, the authors summarized the impact of the 2011 Tohoku earthquake tsunami disaster and discussed the lessons towards the reconstruction of Tohoku region. The 2011 event offers valuable lessons that should be applied in order to build safer and more resilient coastal communities.

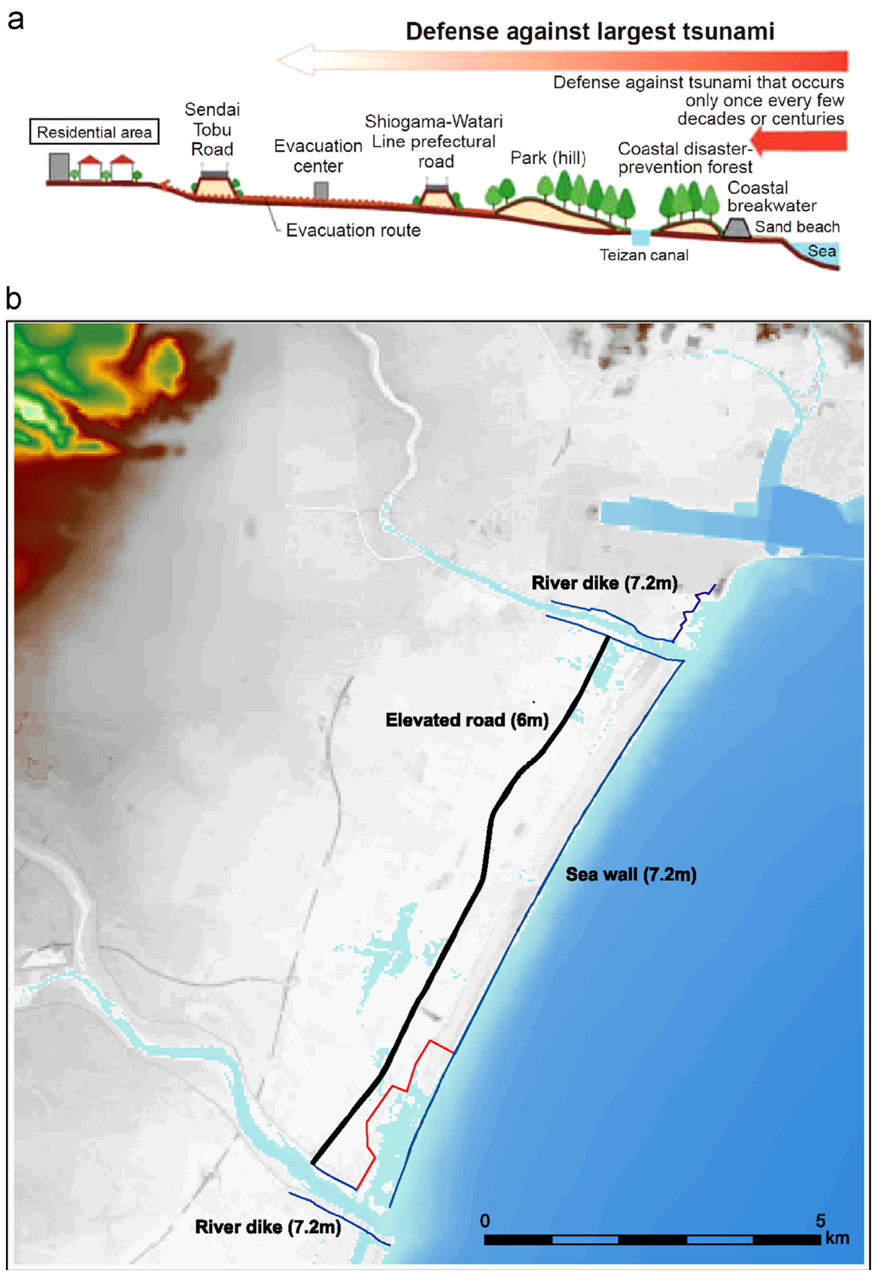

Fig. 12. (a) Conceptual image of tsunami-prevention facilities in Sendai city (2011). (b) Setting of tsunami prevention facilities in Sendai city (2011) reconstruction plan.

As observed in the devastated areas in Miyagi Prefecture, the tsunami flow depth over 2 m has potential to severely damage houses, and more than 6 m flow depth will cause total devastation. This finding can inform land use planning (zoning) or one goal of comprehensive tsunami disaster mitigation, so that residential areas will not be inundated more than 2 m.

The witnessed tsunami front and flow velocities reached approximately 8 m/s on Sendai plain even 1 km inland. The flow velocity of the tsunami inundation in Onagawa town was estimated as 6.3 m/s at the flow depth of approximately 5 m when the houses in the town started being washed-away. At this moment, the tsunami force was roughly estimated as 100 kN/m, the drag force acting on a wall per unit width, and this hydrodynamic force easily destroyed the houses.

Since the 1896 Meiji Sanriku earthquake tsunami that killed 22,000 people, the 1933 Showa earthquake tsunami and since the more recent 1960 Chilean earthquake tsunami, Tohoku region has developed the coastal protection infrastructure of seawalls and breakwaters that have never been devastated throughout the history since 1934. Again, we need to note that coastal infrastructure cannot always protect life and property: even great seawalls may fail. Seawalls should be designed with the assumption of overtopping and resiliency, and communities should not rely on coastal infrastructures alone for protection.

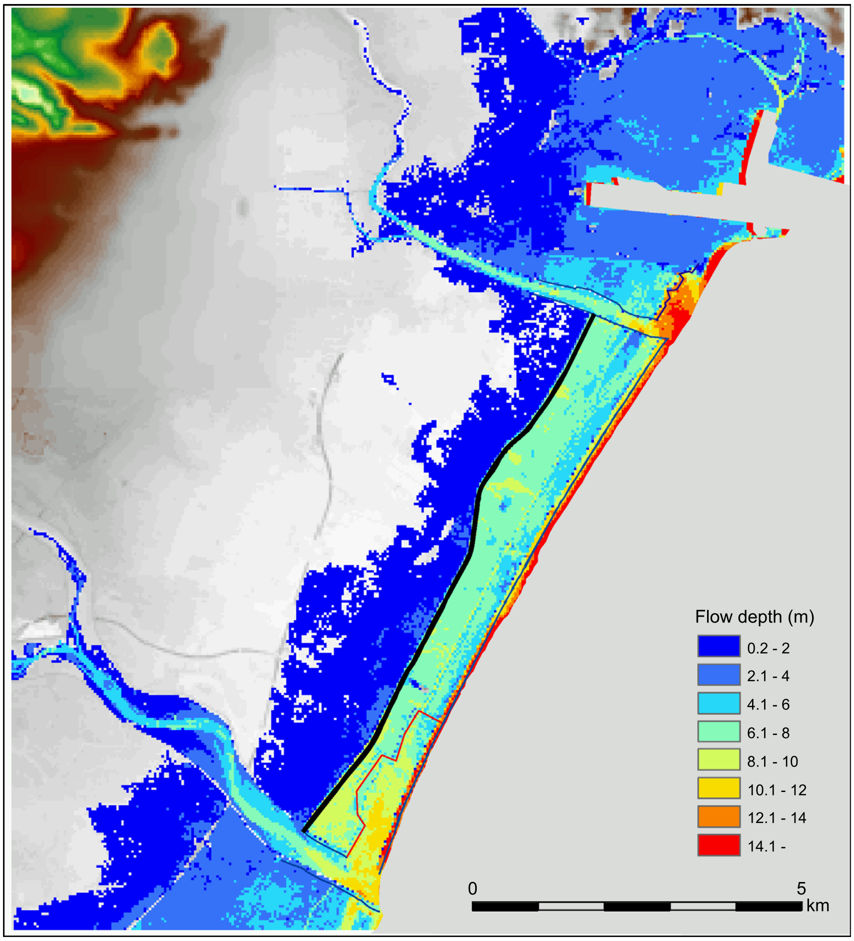

Fig. 13. Preliminary result of tsunami numerical modeling to evaluate the effect of the proposed reconstruction plan in Sendai city (maximum flow depth).

Acknowledgments

This research was funded by the Grant-in-Aid for Scientific Research (Project numbers: 24241059, 24651195 and 22681025) from the Ministry of Education, Culture, Sports, Science and Technology (MEXT) of Japan, IRIDeS project Grant (A-3), and JNES Grant.

References

Abe, I., Abe, T., et al., 2011. High Resolution Survey Results for the Inundation Limit and Height of the 2011 Tohoku Earthquake Tsunami, Abstract of Japan Geoscience Union Meeting 2011, MIS036-P120. 〈http://www2.jpgu.org/meeting/2011/yokou/MIS036-P120.pdf〉.

Cabinet Office. 〈http://www.bousai.go.jp/oshirase/h23/110624-1kisya.pdf〉.

Chock, G., Robertson, I., Kriebel, D., Francis, M., Nistor, I., 2012. Tohoku Japan Tsunami of March 11, 2011 Performance of Structures, ASCE/SEI Tohoku Tsunami Reconnaissance Report.

Gao, B.C., 1996. NDWI—a normalized difference water index for remote sensing of vegetation liquid water from space. Remote Sens. Environ. 58, 257–266.

Geospatial Information Authority of Japan (GSI), 2011a. 〈http://www.gsi.go.jp/〉.

Geospatial Information Authority of Japan (GSI), 2011b. Aerial Photo Archives. 〈http://portal.cyberjapan.jp/denshi/index3_tohoku.html〉.

Gokon, H., Koshimura, S., 2012. Mapping of building damage of the 2011 Tohoku earthquake tsunami in Miyagi Prefecture. Coast. Eng. J. 54 (1), pp. 125006-1-12, http://dx.doi.org/10.1142/S0578563412500064.

Hayashi, S., Koshimura, S., 2013. The 2011 Tohoku tsunami flow velocity estimation by the aerial video analysis and numerical modeling. J. Disaster Res. 8 (4), 561–572.

Imakiire, T., Koarai, M., 2012. Wide-area land subsidence caused by "the 2011 Off the Pacific Coast of Tohoku Earthquake". Soils Found. 52 (5), 842–855.

Japan Aerospace Exploration Agency (JAXA), 2011. 〈http://www.jaxa.jp/press/2011/05/20110512_daichi_e.html〉.

Koshimura, S., Gokon, H., 2012. Structural vulnerability and tsunami fragility curves from the 2011 Tohoku earthquake tsunami disaster. J. Jpn. Soc. Civil Eng. Ser. B2 (Coast. Eng.) 68 (2), 23 I_1421–I_1425 (in Japanese with English abstract).

Koshimura, S., Oie, T., Yanagisawa, H., Imamura, F., 2009. Developing fragility functions for tsunami damage estimation using numerical model and post–tsunami data from Banda Aceh, Indonesia, Coastal Eng. J. 3, 243–273.

Koshimura, S., Namegaya, Y., Yanagisawa, H., 2009b. Tsunami fragility, a new measure to assess tsunami damage. J. Disaster Res. 4 (6), 479–488.

Koshimura, S., Hayashi, S., Gokon, H., 2013. Lessons from the 2011 Tohoku earthquake tsunami disaster. J. Disaster Res. 8 (4), 549–560.

Lei, J., Zhang, L., Wylie, B., 2009. Analysis of dynamic thresholds for the normalized difference water index. Photogramm. Eng. Remote Sens. 75 (11), 1307–1317.

McFeeters, S.K., 1996. The use of the normalized difference water index (NDWI) in the delineation of open water features. Int. J. Remote Sens. 17, 1425–1432.

Ministry of Finance Japan, 2011. Japan's Fiscal Condition. 〈www.mof.go.jp/english/budget/budget/〉.

Ministry of Land, Infrastructure, Transport and Tourism, 2011. 〈http://www.mlit.go.jp/common/000138154.pdf〉.

Mori, N., Takahashi, T., The 2011 Tohoku Earthquake Tsunami Joint Survey Group, 2012. Nationwide post event survey and analysis of the 2011 Tohoku earthquake tsunami, Coastal Eng. J. 54 (1), 125001, http://dx.doi.org/10.1142/S0578563412500015.

National Police Agency, 2012. Report of the Damage Caused by the 2011 Tohoku Earthquake and Tsunami (in Japanese). 〈http://www.npa.go.jp/archive/keibi/biki/higaijokyo.pdf〉.

Rao, G., Lin, A., 2011. Distribution of inundation by the great tsunami of the 2011 Mw 9.0 earthquake off the Pacific coast of Tohoku (Japan), as revealed by ALOS imagery data. Int. J. Remote Sens. 32 (22), 7073–7086.

Sendai city, Sendai City Earthquake Disaster Reconstruction Plan, Digest Version, 2011, 12 pp.

Xu, H., 2006. Modification of normalized difference water index (NDWI) to enhance open water features in remotely sensed imagery. Int. J. Remote Sens. 27, 3015–3033.

Yomiuri Shinbun, 2011. The 2011 tsunami attacking Onagawa town, Miyagi Prefecture (survivor video). 〈www.yomiuri.co.jp/stream/sp/earthquake/earthquake_088.htm〉.